

Adsorption of chromium (VI) by ethylenediamine-modified cross-linked magnetic chitosan resin: Isotherms, kinetics and thermodynamics

Xin-jiang Hu^{a,b}, Jing-song Wang^c, Yun-guo Liu^{a,b,*}, Xin Li^{a,b}, Guang-ming Zeng^{a,b}, Zheng-lei Bao^c, Xiao-xia Zeng^{a,b}, An-wei Chen^{a,b}, Fei Long^{a,b}

^a College of Environmental Science and Engineering, Hunan University, Changsha 410082, PR China

^b Key Laboratory of Environmental Biology and Pollution Control (Hunan University), Ministry of Education, Changsha 410082, PR China

^c School of Urban Construction, University of South China, Hengyang, Hunan 421001, PR China

ARTICLE INFO

Article history:

Received 2 July 2010

Received in revised form 3 September 2010

Accepted 7 September 2010

Available online 17 September 2010

Keywords:

EMCMCR

Chromium (VI)

Adsorption

Equilibrium isotherm

Kinetics

ABSTRACT

The adsorption of chromium (VI) ions from aqueous solution by ethylenediamine-modified cross-linked magnetic chitosan resin (EMCMCR) was studied in a batch adsorption system. Chromium (VI) removal is pH dependent and the optimum adsorption was observed at pH 2.0. The adsorption rate was extremely fast and the equilibrium was established within 6–10 min. The adsorption data could be well interpreted by the Langmuir and Temkin model. The maximum adsorption capacities obtained from the Langmuir model are 51.813 mg g⁻¹, 48.780 mg g⁻¹ and 45.872 mg g⁻¹ at 293, 303 and 313 K, respectively. The adsorption process could be described by pseudo-second-order kinetic model. The intraparticle diffusion study revealed that film diffusion might be involved in the present case. Thermodynamic parameters revealed the feasibility, spontaneity and exothermic nature of adsorption. The sorbents were successfully regenerated using 0.1 N NaOH solutions.

© 2010 Elsevier B.V. All rights reserved.

1. Introduction

Chromium exists in trivalent [Cr (III)] and hexavalent [Cr (VI)] state. The hexavalent form has been considered more hazardous to public health due to its mutagenic and carcinogenic properties [1]. Various methods of chromium removal include filtration, chemical precipitation, adsorption, electrodeposition and membrane systems or even ion exchange process. Among these methods, adsorption is one of the most economically favorable and a technically easy method [2].

Chitosan is the deacetylated form of chitin, which is a linear polymer of acetyl-amino-D-glucose. As chitosan is hydrophilic, biodegradability, harmlessness for living things and ease of chemical derivatization, besides, chitosan has many amino and hydroxyl groups that can chelate heavy metal ions. Therefore, chitosan presents as a very promising starting material for chelating resins [3]. Several metals are preferentially adsorbed in acidic media while chitosan can dissolve in acid condition. To overcome such a problem, some cross-linking agents such as glutaraldehyde [4], epichlorohydrin [5] and ethyleneglycol diglycidyl ether [6] are

used to stabilize chitosan in acid solutions. But glutaraldehyde is the most widely used because it does not have much diminishing adsorption capacity [5]. This method is used to ensure good mechanically and chemically stable beads, but it has been found to have negative effect on the adsorption capacity of the chitosan. The main reason for the loss of adsorption capacity is that amine groups are involved in the cross-linking reaction [7].

The ability of a material to capture metals is controlled in part by the number of available functional groups used for binding metals. The amino and two hydroxyl groups on each glucosamine in the repeating unit of chitosan can act as a reactive site for chemical modification. In order to increase the adsorption ability of chitosan, and to improve the adsorption selectivity of metal ions, several chemicals have been used to modify chitosan such as glycine [8], polydimethylsiloxane [9], thiourea [10] and maleic anhydride [11].

On the other hand, after the adsorption is carried out, the adsorbents are difficult to be separated from the solution using traditional separation methods such as filtration and sedimentation. The magnetic technology is a good solution. Magnetic carriers are used as the support material and they can be easily separated from the reaction medium and stabilized in a fluidized bed reactor by applying a magnetic field [12].

In the present work, we prepared ethylenediamine-modified glutaraldehyde-crosslinked magnetic chitosan resin (EMCMCR) and used it to adsorb Cr (VI) ions in a batch system. The effects of the process parameters such as pH, temperature, dosage of EMCMCR,

* Corresponding author at: College of Environmental Science and Engineering, Hunan University, Changsha 410082, PR China. Tel.: +86 731 88649208; fax: +86 731 88822829.

E-mail address: hnuese@126.com (Y.-g. Liu).

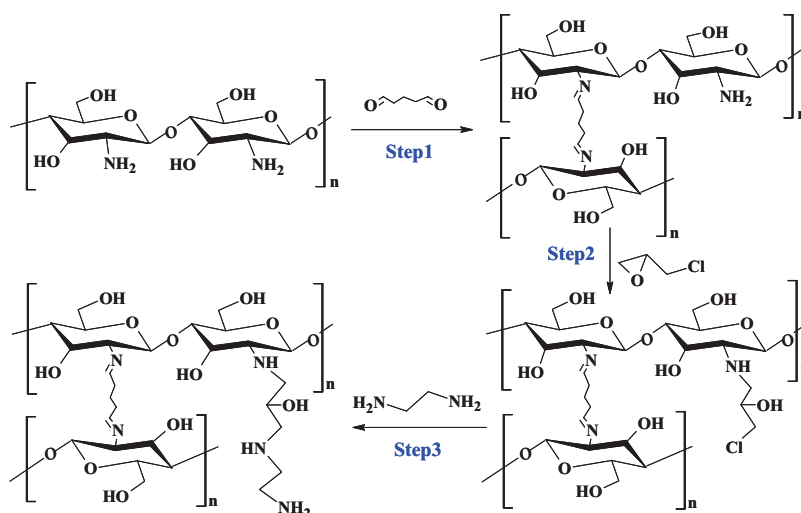


Fig. 1. Scheme for the synthesis of EMCMCR: (step1) expected cross-linking mechanism for chitosan using glutaraldehyde; (step2) expected mechanism of action for cross-linked chitosan using epichlorohydrin; (step3) expected mechanism for aminated chitosan beads.

initial Cr (VI) concentration on Cr (VI) removal were investigated. In order to better understand the adsorption characteristic, some isotherm, kinetic and thermodynamic models were employed to evaluate the sorption process.

2. Materials and methods

2.1. Materials

Chitosan (90% acetylation degree) was supplied by Sinopharm Chemical Reagent Co., Ltd. Glutaraldehyde and epichlorohydrin was provided by Tianjin Guangfu Fine Chemical Research Institute, Tianjin, China. Ethylenediamine was obtained from Changsha Sub-intersection Plastic Chemical Factory, Changsha, China. All reagents above were of Chemical grade.

Stock solutions (1000 mg L^{-1}) of chromium (VI) was prepared by dissolving $2.829 \text{ g K}_2\text{Cr}_2\text{O}_7$ in 1000 mL distilled water. The solutions of different concentrations used in various experiments were obtained by dilution of the stock solutions.

2.2. Preparation of EMCMCR

Magnetic fluid was prepared according to former study [13]. FeCl_3 and FeSO_4 were mixed in the solution with addition of sodium hydroxide to form Fe_3O_4 magnetic particles. The surfactant and the ultrasonic generator were used to disperse the magnetic particles.

EMCMCR was prepared by dissolving chitosan in acetic acid solution with stirring until completely dissolved at 50°C and then the magnetic fluid was added to the solution slowly. Glutaraldehyde and ethylenediamine were used to form the gel. Meanwhile, ethylenediamine was introduced into the mixture to modify the resin. Fig. 1 shows the preparation sketch of EMCMCR. Fig. 2 shows the photos of the chitosan and EMCMCR.

2.3. Batch adsorption experiments

All batch experiments were carried out with adsorbent samples in a 250 mL conical flasks with 100 mL Cr (VI) aqueous solutions on a rotary shaker at 250 r min^{-1} . The concentration of Cr (VI) ions was determined spectrophotometrically at 540 nm using diphenyl carbazide as the complexing agent.

The study of the pH (1.0–8.0) dependency of Cr (VI) adsorption onto EMCMCR was carried out in 100 mL Cr (VI) solutions with different initial concentration of 10 , 60 and 100 mg L^{-1} at a temperature (30°C). The pH value was adjusted by 1 M NaOH or 1 M HCl .

Isotherm studies were conducted by contacting 0.5 g EMCMCR with 100 mL of Cr (VI) solution at different initial concentration (20 , 40 , 60 , 100 and 200 mg L^{-1}) shaking for 60 min . The experiments were performed at different temperature (20 , 30 and 40°C). Sorption isotherms are plots of the equilibrium adsorption capacity (q_e) (according to Eq. (1)) versus the equilibrium concentration of the

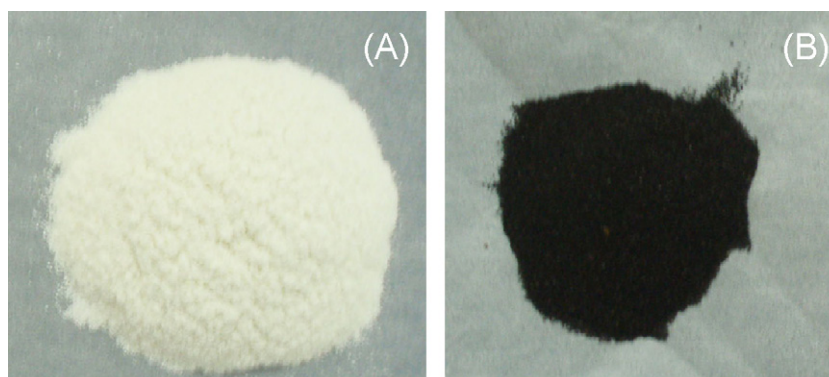


Fig. 2. Photos of chitosan and EMCMCR.

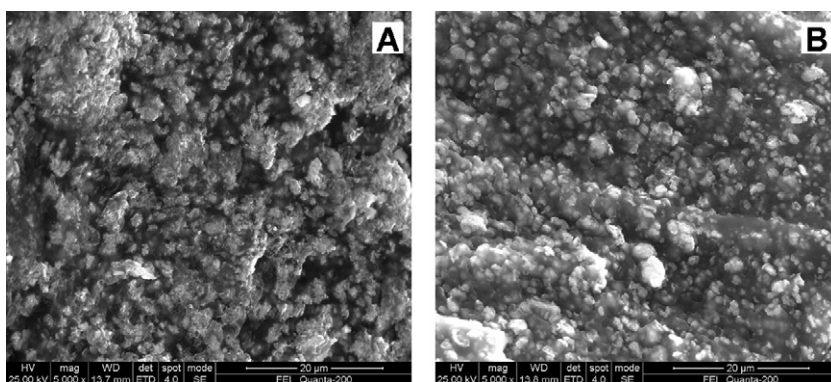


Fig. 3. The SEM characterization of EMCMCR: (A) before (5000 \times) and (B) after (5000 \times) adsorption.

residual Cr (VI) in the solution (C_e).

$$q_e = \frac{(C_0 - C_e)V}{W} \quad (1)$$

where q_e is the equilibrium adsorption capacity (mg g^{-1}), C_0 and C_e are the initial and equilibrium liquid phase solute concentration (mg L^{-1}), respectively. V is the liquid phase volume (L) and W is the amount of adsorbent (g).

To investigate the kinetic characteristics of the adsorption, 0.5 g EMCMCR was added to 100 mL of Cr (VI) solution with three different concentration (60, 100 and 200 mg L^{-1}), and the samples were agitated for designated time periods (2, 4, 6, 8, 10, 20, 30, 40, 50, 60, 90, 120, 150, 180 min).

2.4. Desorption experiments

The adsorption–desorption cycles were repeated consecutively ten times to determine the reusability of sorbents. After adsorption experiments (volume, 100 mL; adsorbent dose, 0.5 g; initial concentration, 300 mg L^{-1} ; pH value, 2; contact time, 60 min; temperature, 30 $^\circ\text{C}$; agitation speed, 250 rpm), the EMCMCR adsorbed with Cr (VI) ions were separated from the solution by filtration and then added into 20 mL various stripping solutions (0.1 M EDTA, 0.1 N HCl, and 0.1 N NaOH, respectively) and stirred at 250 rpm for 30 min at 30 $^\circ\text{C}$ and the final Cr (VI) concentration was determined. After each cycle of adsorption–desorption, sorbent was washed with distilled water and used in the succeeding cycle. The desorption ratio of Cr (VI) ions from EMCMCR was calculated from the amount of Cr (VI) ions adsorbed on EMCMCR and the final Cr (VI) ions concentration in the desorption medium. Desorption ratio was calculated from the following equation:

$$\text{Desorption ratio} = \frac{\text{amount of Cr (VI) ions desorbed to the desorption medium}}{\text{amount of Cr (VI) ions adsorbed onto the EMCECR}} \times 100 \quad (2)$$

3. Results and discussion

3.1. Scanning electron microscope studies

Surface morphology of the EMCMCR before and after adsorption was observed by SEM, and the SEM images are shown in Fig. 3. Before adsorption, irregular surface structure and many pores in the surface were observed, which may exist as amine groups. It is also considered helpful for mass transfer of Cr (VI) ions to EMCMCR. After absorption, the adsorbent surface became abnormal and a great deal of crystal adhered to the surface. These images prove that,

Cr (VI) ion was adsorbed by EMCMCR into its pores and developed a layer of Cr (VI) substance on the surface.

3.2. Effect of pH on Cr (VI) adsorption by EMCMCR

The effect of initial solution pH on Cr (VI) removal by EMCMCR is shown in Fig. 4. The adsorption of Cr (VI) increased with pH increasing from 1.0 to 2.0. The results indicated that at pH 2.0, the maximum adsorption capacity of 2.00, 11.88, 19.76 mg g^{-1} occurred at an initial Cr (VI) concentration of 10, 60 and 100 mg L^{-1} , respectively. Within the range of pH values from 2.0 to 8.0, the adsorption capacity decreased drastically with increasing of pH. This indicates that the adsorption of the adsorbent is clearly pH dependent. Similar trend was also observed with the removal of hexavalent chromium using chitosan derivatives [14], while some researchers have reported the different optimum pH on adsorption of heavy metals by using different kind of modified chitosan. For example, the adsorption of Cr (VI) on CMCB and CMCF was pH dependent and maximum adsorption was obtained at pH 3.0 [15]. The maximum adsorption capacity of the resin QCS for Cr (VI) occurred at a pH value of around 3.5–4.5 [16].

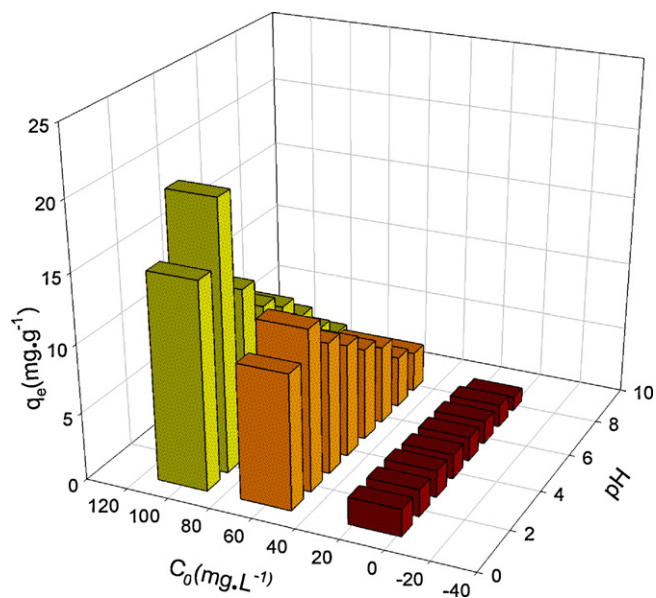


Fig. 4. The effect of initial solution pH on Cr (VI) removal by EMCMCR at various initial concentrations (10, 60 and 100 mg L^{-1}). (Volume, 100 mL; adsorbent dose, 0.5 g; initial concentration, 10, 60 and 100 mg L^{-1} ; pH value, 1, 2, 3, 4, 5, 6, 7, 8; contact time, 60 min; temperature, 303 K; agitation speed, 250 rpm.)

Table 1

Adsorption equilibrium constants obtained from Langmuir, Freundlich and Temkin isotherms in the adsorption of Cr (VI) onto EMCPCR. (Volume, 100 mL; adsorbent dose, 0.5 g; initial concentration, 20, 40, 60, 100, 200 mg L⁻¹; contact time, 60 min; temperature, 293, 303, 313 K; agitation speed, 250 rpm.)

Temperature (°C)	Langmuir model				Freundlich model				Temkin model		
	q_{\max}	K_L	R_L	R^2	n	K_F	q_m	R^2	a_T	b_T	R^2
20	51.813	0.583	0.017	0.997	1.588	16.088	292.349	0.950	7.461	0.238	0.988
30	48.780	0.576	0.017	0.997	1.669	14.763	232.903	0.935	7.284	0.258	0.991
40	45.872	0.522	0.019	>0.999	1.790	12.874	168.699	0.953	6.808	0.293	0.985

It can be explained that because the pH of the aqueous solution affects the speciation of chromium and the surface charge of the adsorbent [17,18]. Cr (VI) exists in different forms in aqueous solution and the stability of these forms is dependent on the pH of the system. At pH 1.0, the chromium ions exist in the form of H₂CrO₄, while in the pH range of 1.0–6.0, different forms of chromium ions such as Cr₂O₇⁻, HCrO₄⁻, Cr₃O₁₀²⁻, Cr₄O₁₃²⁻ co-exist while HCrO₄⁻ predominates. As pH increases, this form shifts to CrO₄²⁻ and Cr₂O₇²⁻ [2]. Cr (VI) exists predominantly as HCrO₄⁻ in aqueous solution below pH 4.0 and the amino groups (-NH₂) of EMCPCR would be in protonated cationic form (-NH₃⁺) to a higher extent in acidic solution which result in a stronger attraction for a negatively charged ion in the solution, and electrostatic interaction occurs between the sorbent and HCrO₄⁻ ions resulting in high chromium removal [19]. However, at pH less than 2.0 a decrease uptake capacity is observed due to the chromium being present predominantly as H₂CrO₄ and a strong competition existed between H₂CrO₄ and protons for adsorption sites. Higher pH decreasing the adsorption capacity may be explained by the dual competition of both the anions (CrO₄²⁻ and OH⁻) to be adsorbed on the surface of the adsorbent of which OH⁻ predominates [2]. Thus, pH of 2.0 was selected as the optimum pH value of Cr (VI) solution for the following adsorption experiment.

3.3. Isotherm studies

Adsorption isotherm studies are important to determine the efficacy of adsorption. Several adsorption isotherms originally used for gas phase adsorption are available and readily adopted to correlate adsorption equilibria in heavy metals adsorption. Some well-known ones are Freundlich, Langmuir, Temkin, Redlich–Paterson and Sips equation [20]. In this study, Langmuir, Freundlich and Temkin models were used to determine the adsorption equilibrium between the adsorbent and metal ions. The isotherm constants for the three models were obtained by linear regression method and presented in Table 1.

The Langmuir model assumes that a monomolecular layer is formed when adsorption takes place without any interaction between the adsorbed molecules [21]. The Langmuir model can be represented as:

$$q_e = \frac{q_{\max} K_L C_e}{1 + K_L C_e} \quad (3)$$

where C_e is the equilibrium concentration (mg L⁻¹), q_e the amount of metal ion sorbed (mg g⁻¹), q_{\max} is q_e for a complete monolayer (mg g⁻¹), K_L is a constant related to the affinity of the binding sites (L mg⁻¹). The linearized form of the Langmuir equation is:

$$\frac{C_e}{q_e} = \frac{1}{q_{\max} K_L} + \frac{C_e}{q_{\max}} \quad (4)$$

The experimental data were plotted as C_e/q_e versus C_e and shown in Fig. 5. The values of Langmuir constants q_{\max} and K_L were obtained by linear regression method and shown in Table 1. The experimental data exhibited high correlation with Langmuir model within the studied temperature range. Both q_{\max} and K_L decreased with increasing temperature, indicating the bonding

between heavy metals and active sites of the adsorbent weakened at higher temperature and the adsorption process is exothermic. This outcome is similar to the studies involving Cr (VI) adsorption on chitosan [19]. But the q_{\max} values obtained for EMCPCR (48.780 mg g⁻¹) at 30 °C is remarkably higher than 7.943 mg g⁻¹ as reported by Aydin et al. [19].

The essential features of a Langmuir isotherm can be expressed in terms of a dimensionless constant separation factor or equilibrium parameter, R_L which is defined by Hall et al. [22] as:

$$R_L = \frac{1}{1 + K_L C_0} \quad (5)$$

where K_L (L mg⁻¹) is the Langmuir constant and C_0 (mg L⁻¹) is the initial concentration. The calculated values of the dimensionless factor R_L are included in Table 1. All R_L values obtained are greater than zero and less than unity indicates the favorable adsorption of Cr (VI) by EMCPCR under consideration. This means that the equilibrium isotherms can be well described by the Langmuir model, and the adsorption process is monolayer adsorption onto a surface with finite number of identical sites, which are homogeneously distributed over the adsorbent surface.

The Freundlich isotherm is an empirical equation assuming that the adsorption process takes place on heterogeneous surfaces and adsorption capacity is related to the concentration of Cr (VI) at equilibrium. This isotherm model is defined by the equation [23] below:

$$q_e = K_F C_e^n \quad (6)$$

where q_e , and C_e are the equilibrium concentrations of chromium (VI) in the adsorbed (mg g⁻¹) and liquid phases (mg L⁻¹), respectively, K_F and n are the Freundlich constants which are related to adsorption capacity and intensity, respectively. This equation can

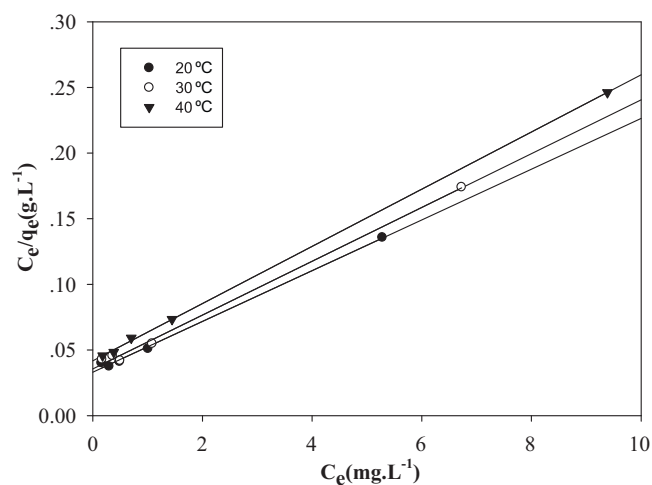


Fig. 5. Langmuir isotherm for the adsorption Cr (VI) ions on EMCPCR. (Volume, 100 mL; adsorbent dose, 0.5 g; initial concentration, 20, 40, 60, 100, 200 mg L⁻¹; contact time, 60 min; temperature, 293, 303, 313 K; agitation speed, 250 rpm.)

be written in the linear form given below:

$$\ln q_e = \frac{1}{n} \ln C_e + \ln K_F \quad (7)$$

To determine the maximum sorption capacity, it is necessary to operate with constant initial concentration C_0 and variable weights of sorbent, thus $\ln q_m$ is the extrapolated value of $\ln q$ for $C = C_0$ [24]. According to Halsey [25]:

$$K_F = \frac{q_m}{C_0^{1/n}} \quad (8)$$

As seen from Table 1, regression correlation coefficients were very high in the temperature range studied. However, the maximum sorption capacity computed using Halsey expression (Table 1) are far higher than the experimental adsorbed amounts at equilibrium corresponding to the plateau of the sorption isotherms. This means that the equilibrium isotherms cannot be described by the Freundlich model.

The derivation of the Temkin isotherm is based on the assumption that the decline of the heat of sorption as a function of temperature is linear rather than logarithmic, as implied in the Freundlich equation. It can be described as follow [26]:

$$q_e = \frac{RT}{b_T} \ln(a_T C_e) = \frac{RT}{b_T} \ln a_T + \frac{RT}{b_T} \ln C_e \quad (9)$$

where a_T is the equilibrium binding constant corresponding to the maximum binding energy (Lg^{-1}), b_T is the Temkin constant related to the heat of sorption (kJ mol^{-1}), and R is the gas constant ($8.314 \times 10^{-3} \text{ kJ mol}^{-1} \text{ K}^{-1}$), T is the absolute temperature (K).

Thus, the constants can be obtained from the slope and intercept of a straight line plot of q_e versus $\ln C_e$. Temkin constants are given in Table 1. Temkin isotherm generates a satisfactory fit to the experimental data as indicated by correlation coefficients. Typical bonding energy range for ion-exchange mechanism is reported to be in the range of 8–16 kJ mol^{-1} while physisorption processes are reported to have adsorption energies less than -40 kJ mol^{-1} [26]. Values of b_T (0.238, 0.258, 0.293 kJ mol^{-1} at an initial concentration of 60, 100 and 200 mg L^{-1} , respectively) obtained in the present study indicates that the adsorption process seems to involve chemisorption and physisorption.

3.4. Kinetic studies

Cr (VI) removal by adsorbent as a function of contact time with different initial concentration (60, 100 and 200 mg L^{-1}) is shown in Fig. 6, where the adsorption rate of metal uptake was very fast and the maximum uptake was observed within 6–10 min. There was almost no further increase of adsorption after 10 min. These results showed that the actual adsorption of metal ion binding to the adsorbent was very rapid. Data on the adsorption rates of Cr (VI) ions by various modified chitosan have shown a wide range of adsorption times. For example, the copper and Cr (VI) adsorption equilibrium time on chitosan derivatives was 2 h [14]. The adsorption equilibrium time of Cr (VI) on the by CMCF and CMCN was 16 h [15].

To investigate the mechanism of adsorption and its potential rate-controlling steps that include mass transport and chemical reaction processes, kinetic models have been exploited to analyse the experimental data. In addition, information on the kinetics of metal uptake is required to select the optimum condition for full-scale batch metal removal processes [20]. Several kinetic models such as pseudo-first-order, pseudo-second-order and intra-particle diffusion model have been applied to find out the adsorption mechanism. The equation of the three kinetic models is expressed as follows:

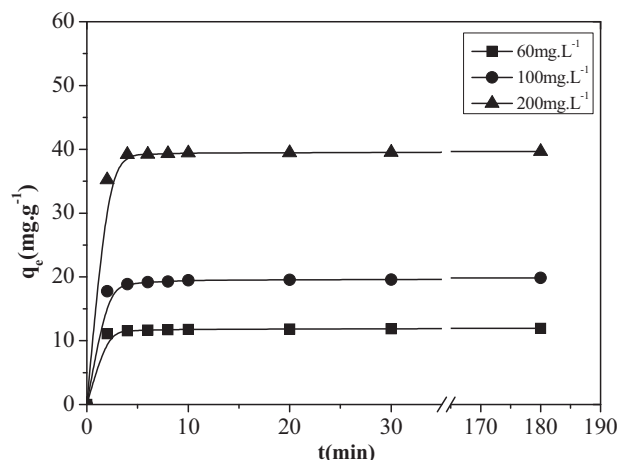


Fig. 6. Effect of contact time on Cr(VI) adsorption. (Volume, 100 mL; adsorbent dose, 0.5 g; initial concentration, 60, 100 and 200 mg L^{-1} ; pH value, 2.0; contact time, 0, 2, 4, 6, 8, 10, 20, 30, 40, 50, 60, 90, 120, 150, 180 min; temperature, 303 K; agitation speed, 250 rpm.)

The first-order rate equation is given as:

$$\log(q_e - q_t) = \log q_e - \frac{k_1}{2.303} t \quad (10)$$

where q_e and q_t are the amounts of adsorbed Cr (VI) on the adsorbent at equilibrium and at time t , respectively (mg g^{-1}), and k_1 is the first-order adsorption rate constant (min^{-1}).

The linearized form of the pseudo-first order model for the sorption of Cr (VI) ions onto EMCMCR at various initial concentrations is given in Fig. 7. The calculated results of the first-order rate equation are given in Table 2. It is found that correlation coefficients values are low, showing the bad quality of linearization. Additionally, the q_e value acquired by this method is contrasted with the experimental value. One suggestion for the differences in experimental and theoretical q_e values is that there is a time lag, possibly due to a boundary layer or external resistance controlling at the beginning of the sorption. This time lag is also difficult to quantify. For this reason, it is necessary to use a trial and error method in order to obtain the equilibrium uptake [27].

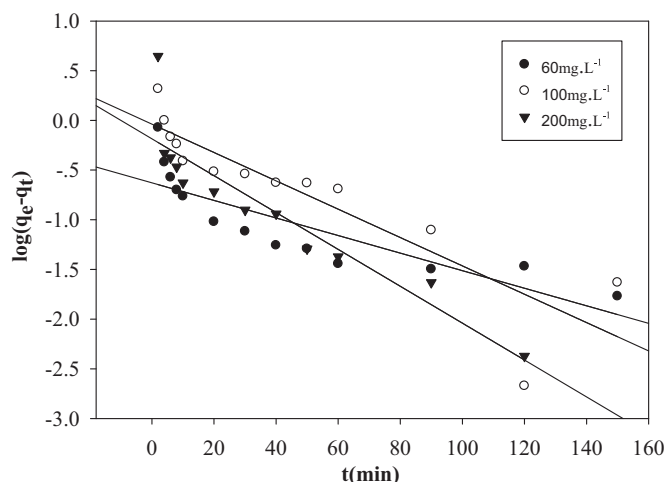


Fig. 7. Pseudo-first order sorption kinetics of Cr (VI) onto EMCMCR at various initial concentrations. (Volume, 100 mL; adsorbent dose, 0.5 g; initial concentration, 60, 100 and 200 mg L^{-1} ; pH value, 2.0; contact time, 0, 2, 4, 6, 8, 10, 20, 30, 40, 50, 60, 90, 120, 150, 180 min; temperature, 303 K; agitation speed, 250 rpm.)

Table 2

Kinetic parameters obtained from Lagrangian models in the adsorption of Cr (VI) onto EMC/MCR. (Volume, 100 mL; adsorbent dose, 0.5 g; initial concentration, 60, 100 and 200 mg L⁻¹; pH value, 2.0; contact time, 0, 2, 4, 6, 8, 10, 20, 30, 40, 50, 60, 90, 120, 150, 180 min; temperature, 303 K; agitation speed, 250 rpm.).

C ₀ (mg L ⁻¹)	Pseudo-first-order			Pseudo-second-order			
	k ₁ (min ⁻¹)	q _e (mg g ⁻¹)	R ²	k ₂ (g mg ⁻¹ min ⁻¹)	q _e (mg g ⁻¹)	h (mg g ⁻¹ min ⁻¹)	R ²
60	0.020	0.235	0.730	0.491	11.933	69.917	>0.999
100	0.033	0.917	0.786	0.140	19.880	55.330	>0.999
200	0.043	0.653	0.844	0.235	39.683	370.064	>0.999

The pseudo-second-order equation is given as:

$$\frac{t}{q_t} = \frac{1}{k_2 q_e^2} + \frac{1}{q_e} t \quad (11)$$

where k_2 is the second-order adsorption rate constant (g mg⁻¹ min⁻¹), and q_e is the adsorption capacity calculated by the pseudo-second-order kinetic model (mg g⁻¹).

The constant k_2 is used to calculate the initial sorption rate h (mg g⁻¹ min⁻¹), at $t \rightarrow 0$ as follows [24]:

$$h = k_2 q_e^2 \quad (12)$$

The linearized form of the pseudo-second order model is given in Fig. 8. The values of the correlation coefficients were all extremely high and all greater than 0.999. Besides, the calculated q_e values agreed very well with the experimental data. Thus experiment results supports the assumption behind the model that the rate limiting step in adsorption of heavy metals are chemisorption involving valence forces through the sharing or exchange of electrons between adsorbent and metal ions. Some studies on the kinetics of Cr (VI) adsorption onto various adsorbents have also reported higher correlations for pseudo-second order model [2,19,28].

The adsorption process on a porous adsorbent will generally have multi-step process. In order to investigate the mechanism of the adsorption of Cr (VI) onto EMC/MCR, the experimental data were tested against the intraparticle diffusion model to identify the mechanism involved in the sorption process. The three consecutive steps in the sorption of a sorbate by a porous sorbent are: (i) mass transfer across the external boundary layer film of liquid surrounding the outside of the particle; (ii) adsorption at a site on the surface (internal or external) and the energy will depend on the binding process (physical or chemical), this step is often assumed to be extremely rapid; (iii) diffusion of the adsorbate molecules to

an adsorption site either by a pore diffusion process through the liquid filled pores or by a solid surface diffusion mechanism [29]. The intraparticle diffusion model can be described as follows [30]:

$$q_t = k_p t^{1/2} + C \quad (13)$$

where k_p is the intra-particle diffusion rate constant (mg g⁻¹ min^{-0.5}) and C of adsorption constant is the intercept. Fig. 9 is the plot of q_t vs. $t^{1/2}$ at different initial Cr (VI) concentration, which indicated that the plot of q_t vs. $t^{1/2}$ was multi-linear, implying that more than one process affected the sorption. Based on these plots, the sorption processes of the three elements are comprised by two phases, suggesting that the intraparticle diffusion is not the rate-limiting step for the whole reaction [31]. The initial portion of the plot indicated an external mass transfer whereas the second linear portion is due to intraparticle or pore diffusion [32].

Due to the double nature of intraparticle diffusion (both film and pore diffusion) (Fig. 6), and in order to determine the actual rate-controlling step involved in the sorption process, the kinetic data have been analyzed using the model given by Boyd et al. [24,33]

$$F = 1 - \frac{6}{\pi^2} \sum_{m=1}^{\infty} \frac{1}{m^2} \exp \left[\frac{-D_i \pi^2 m^2 t}{r^2} \right] \quad (14)$$

or

$$F = 1 - \frac{6}{\pi^2} \sum_{m=1}^{\infty} \frac{1}{m^2} \exp(-m^2 Bt) \quad (15)$$

where F is the fractional attainment of equilibrium at time t and is obtained by the expression:

$$F = \frac{q_t}{q_e} \quad (16)$$

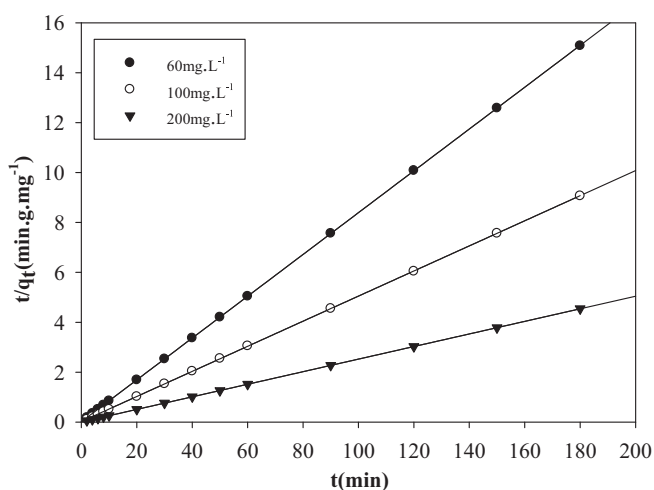


Fig. 8. Pseudo-second order sorption kinetics of Cr (VI) onto EMC/MCR at various initial concentrations. (Volume, 100 mL; adsorbent dose, 0.5 g; initial concentration, 60, 100 and 200 mg L⁻¹; pH value, 2.0; contact time, 0, 2, 4, 6, 8, 10, 20, 30, 40, 50, 60, 90, 120, 150, 180 min; temperature, 303 K; agitation speed, 250 rpm.)

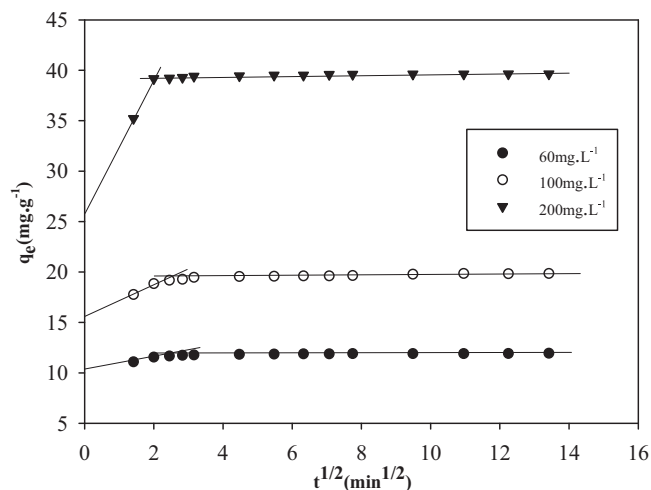


Fig. 9. Intraparticle diffusion kinetics of Cr (VI) onto EMC/MCR at various initial concentrations. (Volume, 100 mL; adsorbent dose, 0.5 g; initial concentration, 60, 100 and 200 mg L⁻¹; pH value, 2.0; contact time, 0, 2, 4, 6, 8, 10, 20, 30, 40, 50, 60, 90, 120, 150, 180 min; temperature, 303 K; agitation speed, 250 rpm.)

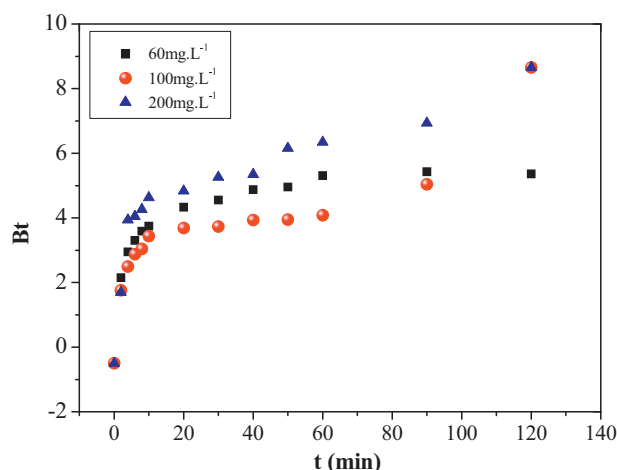


Fig. 10. Boyd plot for Cr(VI) sorption onto EMCMCR at various initial concentrations (60, 100 and 200 mg L⁻¹). (Volume, 100 mL; adsorbent dose, 0.5 g; initial concentration, 60, 100 and 200 mg L⁻¹; pH value, 2.0; contact time, 0, 2, 4, 6, 8, 10, 20, 30, 40, 50, 60, 90, 120, 150, 180 min; temperature, 303 K; agitation speed, 250 rpm.)

where q_t (mg g⁻¹) is the amount of sorbate taken up at time t and q_e (mg g⁻¹) is the maximum equilibrium uptake and

$$B = \frac{D_i \pi^2}{r^2} \quad (17)$$

where B is the time constant (min⁻¹), D_i is the effective diffusion coefficient of the metal ions in the sorbent phase (cm² min⁻¹), r is the radius of the sorbent particle (cm), assumed to be spherical, and m is an integer that defines the infinite series solution. Bt is given by the equation:

$$Bt = -0.4977 - \ln(1 - F) \quad (18)$$

Thus, the value of Bt can be computed for each value of F , and then plotted against time to configure the so-called Boyd plots. The linearity plot of Bt vs. t plots (Fig. 10) was employed to distinguish between sorption controlled by film diffusion and particle diffusion [24]. A straight line passing through the origin is indicative of sorption processes governed by particle-diffusion mechanisms. Otherwise they are governed by film diffusion [34]. From Fig. 10, it was observed that the plots were neither linear nor passed through the origin at various initial concentrations, indicating the film-diffusion-controlled mechanism. Usually, external transport is the rate-limiting step in systems, which have poor mixing, dilute concentration of adsorbate, small particle size and high affinity of adsorbate for adsorbent. In contrast, the intraparticle step limits the overall transfer for those systems that have high concentration of adsorbate, good mixing, large particle size of adsorbent and low affinity of adsorbate for adsorbent [35]. In our research, the strong external resistance which hinders the external mass transfer may be due to the poor mixing (agitation speed 250 rpm), low concentration of adsorbate (initial concentration, 60, 100 and 200 mg L⁻¹, respectively, but low concentration remained when the intraparticle-diffusion takes control of the adsorption rate) and small particle sizes of EMCMCR (particle sizes below 300 μm). Besides, the adsorbate displays higher affinity for the EMCMCR, which results in low internal resistance. Because the overall rate of sorption will be controlled by the slowest step (higher resistance step)[35], so the external mass transport (film diffusion) mainly governs the intraparticle diffusion in our study. Similar results were obtained by Aguilar-Carrillo et al. [32].

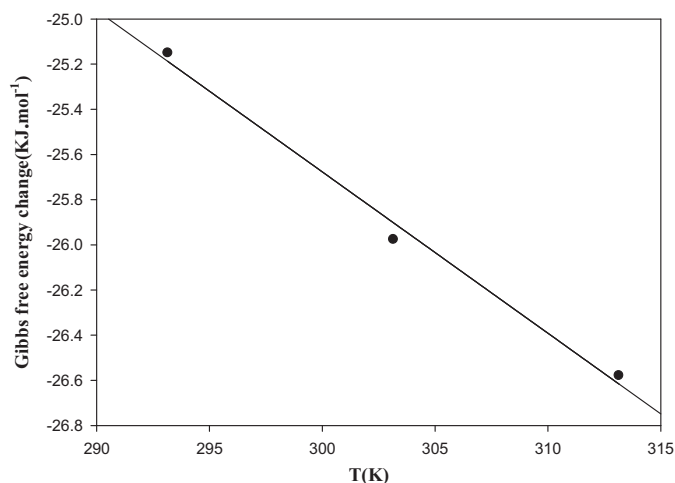


Fig. 11. plot of Gibbs free energy change, ΔG° versus temperature, T . (Volume, 100 mL; adsorbent dose, 0.5 g; initial concentration, 20, 40, 60, 100, 200 mg L⁻¹; contact time, 60 min; temperature, 293, 303, 313 K; agitation speed, 250 rpm.)

3.5. Thermodynamic studies

Thermodynamic considerations of an adsorption process are necessary to conclude whether the process is spontaneous or not. The experimental data obtained at different temperatures were used in calculating the thermodynamic parameters such as Gibbs free energy change (ΔG°), enthalpy change (ΔH°) and entropy change (ΔS°). The Gibbs free energy change of the sorption reaction is given by the following [36]:

$$\Delta G^\circ = -RT \ln K_L \quad (19)$$

$$\Delta G^\circ = \Delta H^\circ - T\Delta S^\circ \quad (20)$$

where K_L is the equilibrium constant, which can be obtained from Langmuir isotherms at different temperature, R is the universal gas constant, 8.314 J mol⁻¹ K⁻¹, and T is absolute temperature (K). ΔH° and ΔS° were obtained from the slope and intercept of the plot of Gibbs free energy change, ΔG° vs. temperature, T (Fig. 11). The calculated results are reported in Table 3.

The negative values of ΔG° confirm the feasibility of the process and the spontaneous nature of adsorption with a high preference for Cr(VI) onto EMCMCR. The standard enthalpy and entropy changes of adsorption determined from Fig. 11 were -4.242 kJ mol⁻¹ and 71.450 J mol⁻¹ K⁻¹, respectively, with a correlation coefficient of 0.992. The value of ΔH° is negative, indicating that the adsorption reaction is exothermic. The positive value of ΔS° reflects an increase in the randomness at the solid/solution interface during the adsorption process [37].

3.6. Desorption studies

Desorption was carried out with EDTA, HCl, and NaOH. It was observed that only 69.76% of the loaded Cr(VI) stripped in 0.1 M EDTA and 15.19% stripped with 0.1 N HCl, while 87.96% stripped with 0.1 N NaOH in the first cycle. Perhaps due to the speciation of chromium and the surface charge of the adsorbent have changed into the alkaline medium which would weaken the electrostatic interaction between the EMCMCR and the Cr(VI) ions, promoting desorption. Hence, further experiments were carried out only with 0.1 N NaOH solutions. Complete desorption was not possible, perhaps due to the involvement of non-electrostatic forces between the EMCMCR and the Cr(VI) ions [38]. The regenerated EMCMCR was reused for up to 10 adsorption-desorption cycles and the results are illustrated in Fig. 12. It was found that the adsorp-

Table 3

Thermodynamic parameters for the adsorption of Cr (VI) on EMCPCR at different temperatures. (Volume, 100 mL; adsorbent dose, 0.5 g; initial concentration, 20, 40, 60, 100, 200 mg L⁻¹; contact time, 60 min; temperature, 293, 303, 313 K; agitation speed, 250 rpm.).

Temperature (°C)	K_L (L mg ⁻¹)	ΔG° (KJ mol ⁻¹)	ΔH° (KJ mol ⁻¹)	ΔS° (JK ⁻¹ mol ⁻¹)	R^2
20	0.583	-25.150	-4.242	71.450	0.992
30	0.576	-25.976			
40	0.522	-26.579			

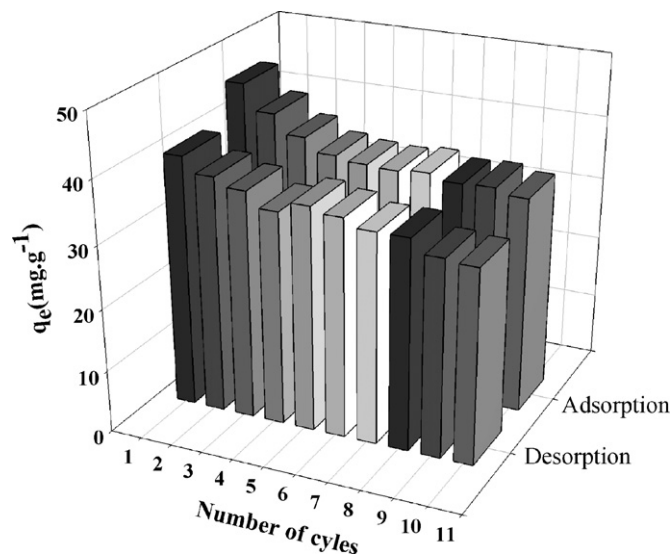


Fig. 12. Adsorption–desorption cycles for EMCPCR. (Adsorption conditions: volume, 100 mL; adsorbent dose, 0.5 g; initial concentration, 300 mg L⁻¹; contact time, 60 min; temperature, 303 K; agitation speed, 250 rpm. Desorption conditions: tripping solution 0.1 N NaOH; volume, 20 mL; contact time, 30 min; temperature, 303 K; agitation speed, 250 rpm.)

tion capacity of the EMCPCR was an 8.87% decrease after the first cycle and a 15.40% decrease after the second cycle. It could still be maintained at 75.73% level at the 10th cycle. These results showed that the EMCPCR can be successfully regenerated and repeatedly used in Cr (VI) ions adsorption studies without appreciable losses in their adsorption capacities.

4. Conclusions

The present study focuses on adsorption of Cr (VI) from aqueous solution using the EMCPCR as an effectively adsorbent. Adsorption of Cr (VI) is found to be effective in the lower pH range and at lower temperatures. In addition, the very fast adsorption and settling for the EMCPCR make this material suitable for continuous flow water treatment systems. Equilibrium isotherm data were fitted using different two-parameter models. Among these models, Langmuir model and Temkin model are in good agreement with the experimental data with high R^2 . Kinetic study showed that the pseudo-second order model is appropriate to describe the experimental and film diffusion might be involved in the sorption process. The adsorption of Cr (VI) dependence on temperature was investigated and the thermodynamic parameters ΔG° , ΔH° and ΔS° were calculated. The results show a feasible, spontaneous and exothermic adsorption process. The mechanism of adsorption includes mainly ionic interactions (chemical interactions) and electrostatic interactions (physical interactions) between metal cations and EMCPCR. So the adsorption is a physicochemical process. The adsorption–desorption cycle results demonstrated that the regeneration and subsequent use the EMCPCR would enhance the economics of practical applications for the removal of Cr (VI) from water and wastewater.

Acknowledgements

The authors would like to thank financial support from the National Natural Science Foundation of China (Grant nos. 20707008 and 10775065) and the Scientific Research Fund of Hunan Provincial Education Department (Grant no. 06B082) and the Hunan University ability training projects by the basic operation costs of central Colleges and Universities for Scientific Research (Grant no. hdzy0903).

References

- [1] S. Basha, Z.V.P. Murthy, B. Jha, Biosorption of hexavalent chromium by chemically modified seaweed, *Cystoseira indica*, Chem. Eng. J. 137 (2008) 480–488.
- [2] T. Karthikeyan, S. Rajgopal, L.R. Miranda, Chromium (VI) adsorption from aqueous solution by Hevea Brasiliensis sawdust activated carbon, J. Hazard. Mater. B124 (2005) 192–199.
- [3] N.G. Kandile, A.S. Nasr, Environment friendly modified chitosan hydrogels as a matrix for adsorption of metal ions, synthesis and characterization, Carbohydr. Polym. 78 (2009) 753–759.
- [4] M. Ruiz, A.M. Sastre, E. Guibal, Palladium sorption on glutaraldehyde-crosslinked chitosan, React. Funct. Polym. 45 (2000) 155–173.
- [5] W.S.W. Ngah, C.S. Endud, R. Mayanar, Removal of copper(II) ions from aqueous solution onto chitosan and cross-linking chitosan beads, React. Funct. Polym. 20 (2002) 181–190.
- [6] N. Li, R. Bai, Development of chitosan-based granular adsorbents for enhanced and selective adsorption performance in heavy metal removal, Wat. Sci. Technol. 54 (2006) 103–113.
- [7] L. Martinez, F. Agnely, B. Leclerc, J. Siepmann, M. Cotte, S. Deiger, G. Couarraze, Cross-linking of chitosan and chitosan poly(ethylene oxide) beads: a theoretical treatment, Eur. J. Pharm. Biopharm. 67 (2007) 339–348.
- [8] A. Ramesh, H. Hasegawa, W. Sugimoto, T. Maki, K. Ueda, Adsorption of gold(III), platinum(IV) and palladium(II) onto glycine modified crosslinked chitosan resin, Bioresour. Technol. 99 (2008) 3801–3809.
- [9] M. Rutnakornpituk, P. Ngamdee, P. Phinyocheep, Preparation and properties of polydimethylsiloxane-modified chitosan, Carbohydr. Polym. 63 (2006) 229–237.
- [10] L. Zhou, Y. Wang, Z. Liu, Q. Huang, Characteristics of equilibrium, kinetics studies for adsorption of Hg(II), Cu(II), and Ni(II) ions by thiourea-modified magnetic chitosan microspheres, J. Hazard. Mater. 161 (2009) 995–1002.
- [11] T.Y. Guo, Y.Q. Xia, G.J. Hao, B.H. Zhang, G.Q. Fu, Z. Yuan, B.L. He, J.F. Kennedy, Chemically modified chitosan beads as matrices for adsorptive separation of proteins by molecularly imprinted polymer, Carbohydr. Polym. 62 (2005) 214–221.
- [12] E.B. Denkbaz, E. Kiliçay, C. Birlikseven, E. Öztürk, Magnetic chitosan microspheres: preparation and characterization, React. Funct. Polym. 50 (2002) 225–232.
- [13] Z.L. Bao, J.S. Wang, J.H. Liu, L.P. Liu, Preparation of water-based Fe₃O₄ magnetic fluids via chemical co-precipitation as precursors of complex adsorbent, in: 2009 International Symposium on Environmental Science and Technology, Shanghai, China, June 2–5, 2009, pp. 1585–1591.
- [14] G.Z. Kyzas, M. Kostoglou, N.K. Lazaridis, Copper and chromium (VI) removal by chitosan derivatives—equilibrium and kinetic studies, Chem. Eng. J. 152 (2009) 440–448.
- [15] N. Sankaramakrishnan, A. Dixit, L. Iyengar, R. Sanghi, Removal of hexavalent chromium using a novel cross linked xanthated chitosan agent, Bioresour. Technol. 97 (2006) 2377–2382.
- [16] V.A. Spinelli, M.C.M. Laranjeira, V.T. Fávère, Preparation and characterization of quaternary chitosan salt: adsorption equilibrium of chromium (VI) ion, React. Funct. Polym. 61 (2004) 347–352.
- [17] S.M. Nomanbhay, K. Palanisamy, Removal of heavy metal from industrial wastewater using chitosan coated oil palm shell charcoal, Electron. J. Biotechnol. 8 (2005) 43–53.
- [18] S.J. Park, Y.S. Jang, Pore structure and surface properties of chemically Modified activated carbons for adsorption mechanism and rate of Cr(VI), J. Colloid Interface Sci. 249 (2002) 458–463.
- [19] Y.A. Aydın, N.D. Aksoy, Adsorption of chromium on chitosan: optimization, kinetics and thermodynamics, Chem. Eng. J. 151 (2009) 188–194.
- [20] J. Febrianto, A.N. Kosasih, J. Sunarso, Y.H. Ju, N. Indraswati, S. Ismadji, Equilibrium and kinetic studies in adsorption of heavy metals using biosorbent: a summary of recent studies, J. Hazard. Mater. 162 (2009) 616–645.

- [21] Z. Aksu, Determination of the equilibrium, kinetic and thermodynamic parameters of the batch biosorption of nickel (II) ions onto *Chlorella vulgaris*, *Process Biochem.* 38 (2002) 89–99.
- [22] K.R. Hall, L.C. Eagleton, A. Acrivos, T. Vermeulen, Pore- and solid-diffusion kinetics in fixed-bed adsorption under constant pattern conditions, *Ind. Eng. Chem. Fundam.* 5 (1966) 212–223.
- [23] Y.H. Li, Z. Di, J. Ding, D. Wu, Z. Luan, Y. Zhu, Adsorption thermodynamic, kinetic and desorption studies of Pb^{2+} on carbon nanotubes, *Water Res.* 39 (2005) 605–609.
- [24] R. Djeribi, O. Hamdaoui, Sorption of copper (II) from aqueous solutions by cedar sawdust and crushed brick, *Desalination* 225 (2008) 95–112.
- [25] G.D. Halsey, The role of surface heterogeneity in adsorption, *Adv. Catal.* 4 (1952) 259–269.
- [26] B. Kiran, A. Kaushik, Chromium binding capacity of *Lyngbya putealis* exopolysaccharides, *Biochem. Eng. J.* 38 (2008) 47–54.
- [27] Y. Säg, Y. Aktay, Kinetic studies on sorption of Cr(VI) and Cu(II) ions by chitin, chitosan and *Rhizopus arrhizus*, *Biochem. Eng. J.* 12 (2002) 143–153.
- [28] C. Qin, Y. Du, Z. Zhang, Y. Liu, L. Xiao, X. Shi, Adsorption of chromium (VI) on a novel quaternized chitosan resin, *J. Appl. Polym. Sci.* 90 (2003) 505–510.
- [29] W.H. Cheung, Y.S. Szeto, G. McKay, Intraparticle diffusion processes during acid dye adsorption onto chitosan, *Bioresour. Technol.* 98 (2007) 2897–2904.
- [30] S. Basha, Z.V.P. Murthy, B. Jha, Sorption of Hg (II) onto *Carica papaya*: experimental studies and design of batch sorber, *Chem. Eng. J.* 147 (2009) 226–234.
- [31] Y.S. Ho, A.E. Ofomaja, Kinetics and thermodynamics of lead ion sorption on palm kernel fibre from aqueous solution, *Process Biochem.* 40 (2005) 3455–3461.
- [32] J. Aguilar-Carrillo, F. Garrido, L. Barrios, M.T. Garcia-Gonzalez, Sorption of As Cd and Tl as influenced by industrial by-products applied to an acidic soil: equilibrium and kinetic experiments, *Chemosphere* 65 (2006) 2377–2387.
- [33] G.E. Boyd, A.W. Adamson, L.S. Myers, The exchange adsorption of ions from aqueous solutions by organic zeolites, *J. Am. Chem. Soc.* 69 (1947) 2836–2848.
- [34] D. Mohan, K.P. Singh, Single- and multi-component adsorption of cadmium and zinc using activated carbon derived from bagasse—an agricultural waste, *Water Res.* 36 (2002) 2304–2318.
- [35] V. Vadivelan, K.V. Kumar, Equilibrium, kinetics, mechanism, and process design for the sorption of methylene blue onto rice husk, *J. Colloid Interface Sci.* 286 (2005) 90–100.
- [36] T. Fan, Y.G. Liu, B.Y. Feng, G.M. Zeng, C.P. Yang, M. Zhou, H.Z. Zhou, Z.F. Tan, X. Wang, Biosorption of cadmium(II), zinc(II) and lead(II) by *Penicillium simplicissimum*: isotherms, kinetics and thermodynamics, *J. Hazard. Mater.* 160 (2008) 655–661.
- [37] W.S.W. Ngah, S. Fatinathan, Adsorption of Cu(II) ions in aqueous solution using chitosan beads, chitosan-GLA beads and chitosan-alginate beads, *Chem. Eng. J.* 143 (2008) 62–72.
- [38] V. Singh, S. Tiwari, A.K. Sharma, R. Sanghi, Removal of lead from aqueous solutions using *Cassia grandis* seed gum-graft-poly(methylmethacrylate), *J. Colloid Interface Sci.* 316 (2007) 224–232.